International Journal of Pharmaceutics 403 (2011) 96–100

Contents lists available at ScienceDirect

International Journal of Pharmaceutics

journal homepage: www.elsevier.com/locate/ijpharm

Solubility and partitioning of carbamazepine in a two-phase supercritical carbon dioxide/polyvinylpyrrolidone system

Shweta Ugaonkar[a], Thomas E. Needham[a], Geoffrey D. Bothun[b,*]

[a] Department of Biomedical and Pharmaceutical Sciences, University of Rhode Island, Kingston, RI 02881, United States
[b] Department of Chemical Engineering, University of Rhode Island, 16 Greenhouse Rd, RI 02881, United States

ARTICLE INFO

Article history:
Received 16 August 2010
Received in revised form 12 October 2010
Accepted 18 October 2010
Available online 30 October 2010

Keywords:
Carbamazepine
Supercritical
Excipient
Formulation
Polymer swelling
Drug partitioning

ABSTRACT

Supercritical carbon dioxide ($scCO_2$) processing of drug/polymer mixtures is an environmentally friendly means of creating an impregnated polymeric carrier to enhance the aqueous dissolution rate of drugs that exhibit poor water solubility or are thermally labile. However, the role of drug solubilization and its interaction with the polymer during $scCO_2$ processing on the extent and rate of dissolution has been ambiguous. In this study, we examine the rate of dissolution of carbamazepine (CBZ), a hydrophobic drug for treating epilepsy, in $scCO_2$ (90–200 bar, 35 °C and 45 °C) and its partitioning into polyvinylpyrrolidone (PVP, 10 and 29 K MW) using *in situ* UV–vis spectroscopy. Our results show that partitioning occurs by surface adsorption and impregnation within the polymer matrix. These processes are linked to plasticization, which is dependent on PVP molecular weight, and temperature and pressure during treatment. The rate and extent of CBZ solubility is also controlled by treatment condition. The ability to tune polymer and drug simultaneously can be used to control the nature and extent of drug loading.

1. Introduction

Formulation of a water insoluble drug faces several challenges owing to the inherent properties of the drug itself, including crystallinity and hydrophobicity, which restricts free dissolution in water. Non-crystalline amorphous forms can be formed, which improve the dissolution rate, but these forms are thermodynamically unstable and ultimately convert back to more stable crystalline forms (Craig et al., 1999). Carbamazepine (CBZ), a class II compound as per the Biopharmaceutics Classification system (Lőbenberg and Amidon, 2000), is one such crystalline drug that would greatly benefit from an improved dissolution rate as its absorption from the gastrointestinal tract is dissolution-limited (Nair et al., 2002). In order to circumvent thermodynamic instability posed by amorphous forms, another common route that is adopted to enhance the solubility and rate of dissolution of drugs is to combine them with water soluble, pharmaceutically acceptable polymer excipients. This is commonly achieved using melt dispersion, spray drying, or film coating techniques (Hancock et al., 1995; Hancock and Zografi, 1997). Amorphous forms, if generated, are stabilized by co-solidifying the drug with the polymer excipients. This hampers the molecular mobility of the drug and prolongs the amorphous to crystalline conversion (Yoshioka et al., 1995; Hancock et al., 1995).

In the case of CBZ, a remarkable increase in aqueous CBZ dissolution has been reported when formulated with water-soluble polymer solid dispersions, which led to increased bioavailability (El-Zein et al., 1998). Examples of the polymeric pharmaceutical excipients used include polyvinylpyrrolidone (PVP), hydroxypropyl methylcellulose (HPMC), and polyethylene glycol (PEG). However, a major limitation associated with utilizing such polymers is that conventional processing techniques generally require the use of organic solvents that pose a toxicological threat. Also, some drugs are thermally labile and the formation of drug–polymer mixtures must be accomplished using non-thermal processes. This limits the types of processing techniques that can be employed.

Liquid or supercritical carbon dioxide-based solvent systems can be used as an alternative method to prepare and process drug-impregnated polymer mixtures without the use of organic solvents. There are several advantages to employing carbon dioxide as a solvent; it is non-flammable, chemically inert, inexpensive, and has an accessible critical temperature (31 °C) and critical pressure (73.8 bar) (Hyatt, 1984; McHugh and Krukonis, 1994). CO_2 is also environmentally friendly as it can be removed from the atmosphere and recycled in a closed-loop process. A key property of $scCO_2$ is the ability to tune solvent strength and mass transfer properties with slight changes in the pressure or temperature (Mukhopadhyay, 2004). CO_2 is widely applicable in the pharmaceutical industry and it can plasticize amorphous polymers, which mimics heat-induced plasticization (Kazarian et al., 1997; Kazarian, 2000, 2004). Hence, CO_2-based processes for creating drug–polymer mixtures are of great interest (Moneghini et al., 2001; Sethia and Squillante, 2004;

* Corresponding author. Tel.: +1 401 874 9518; fax: +1 401 874 4689.
E-mail address: bothun@egr.uri.edu (G.D. Bothun).

0378-5173/$ – see front matter © 2010 Elsevier B.V. All rights reserved.
doi:10.1016/j.ijpharm.2010.10.031

Nomenclature

CBZ	carbamazepine
PVP	polyvinylpyrrolidone
$A_{280\,nm}$	absorbance at 280 nm
a_D	molar adsorptivity (mol mol^{-1} cm^{-1})
b	light pathlength (cm)
K_D	drug (CBZ) partition coefficient (mole fraction basis)
$m_D^{CO_2}$	mass of drug in CO_2
m_D^{PVP}	mass of drug in PVP
M_D	total mass of drug
MW_D	molecular weight of drug
$MW_{N\text{-}VP}$	molecular weight of PVP monomer (N-vinylpyrrolidone)
$x_D^{CO_2}$	mole fraction of drug in CO_2
x_D^{PVP}	mole fraction of drug in PVP

Kikic and Vecchione, 2003; Kazarian and Martirosyan, 2002; Guney and Akgerman, 2002; Senčar-Božič et al., 1997).

CO_2 plays a dual role in forming drug-impregnated polymer mixtures. It plasticizes the amorphous polymer (Kikic et al., 1999; Kikic and Vecchione, 2003; Shieh et al., 1996) and it fully or partially solubilizes the drug, as illustrated in Fig. 1. For a given polymer, the impregnation of a drug within the polymer is influenced by its degree of plasticization by CO_2, which is a function of the polymer molecular weight, the drug solubility in CO_2, and the drug partitioning between CO_2 and the polymer phase. These properties are functions of temperature and pressure, and further influenced by the processing duration. If ample time is given for plasticization and drug solubilization, a drug that exhibits a high affinity for the polymer phase can quickly sorb into the polymer matrix. Alternatively, if the drug shows a greater affinity for the scCO_2 phase, impregnation of the polymer often occurs by drug deposition within the plasticized matrix upon depressurization. This could result in the re-crystallization of the solute rather than yielding the desired molecularly dispersed solute within the polymer matrix (Kazarian and Martirosyan, 2002), which can impair aqueous drug dissolution.

Results from our previous work (Ugaonkar et al., 2007), where PVP–CBZ mixtures were processed as a function of PVP molecular weight (10 and 29 K) in near- and supercritical CO_2, suggest that a combined effect of PVP plasticization and CBZ dissolution in CO_2 are critical in controlling the nature of the PVP–CBZ interaction and achieving enhanced aqueous dissolution of CBZ. In this work we have measured CBZ scCO_2/PVP partition coefficients as functions of temperature (35 °C and 45 °C) and PVP MW (10 and 29 K) using *in situ* UV–vis spectroscopy. Our objective was to examine the relationship between PVP morphology and CBZ partitioning to determine whether CBZ partitioning was driven by absorption or adsorption.

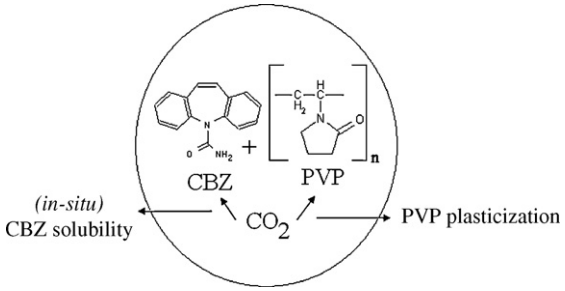

Fig. 1. Schematic of depicting the effects of *in situ* CO_2 processing of CBZ/PVP.

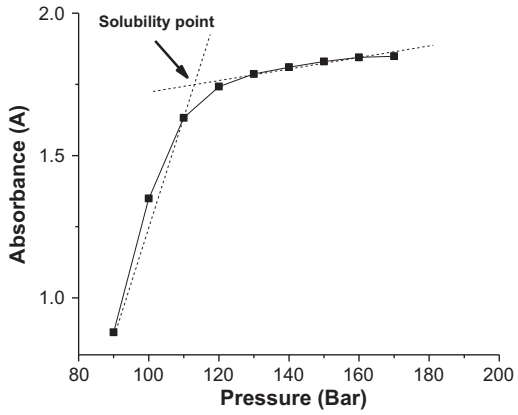

Fig. 2. Representative plot depicting the graphical method used to determine equilibrium solubility. UV absorbance of CBZ (0.2 mg in 12 ml of CO_2) is plotted as a function of pressure at 35 °C. A solubility of 4.26×10^{-6} mol/mol is taken from the solubility point intercept at the set pressure.

2. Materials and methods

2.1. Materials

Carbon dioxide (99.8% purity, bone dry grade) was procured from Airgas (East Greenwich, RI). Carbamazepine in monoclinic form was a gift from Hitech Pharmacal (Amityville, NY). Polyvinylpyrrolidone 10 K and 29 K were purchased from Sigma–Aldrich (St. Louis, MO).

2.2. CBZ dissolution, solubility, and partitioning behavior

The *in situ* high-pressure UV–vis spectroscopy technique used to measure CBZ absorbance was adapted from Ngo et al. (2001). The advantages of this technique are that it does not require external sampling, it is particularly useful for solutes at low concentrations, it eliminates the need to account for density dependent changes in solute molar absorptivities in scCO_2 (Rice et al., 1995), and it does not require prior knowledge of molar absorptivity to obtain solute concentration. The effects of temperature, pressure, and the presence of PVP on the rate of dissolution of CBZ in the scCO_2 phases are clearly demonstrated using this method.

CBZ solubility measurements were conducted by placing a known amount of dry CBZ powder in a high-pressure spectroscopic cell (~12 ml internal volume; Thar Technologies, Pittsburg, PA). The cell was sealed, placed inside a UV–vis spectrophotometer (Cary 50, Varian Inc., Palo Alto, CA), and slowly loaded with liquid CO_2 using an ISCO syringe pump (model 500D, Teledyne-ISCO, Lincoln, NE). The liquefied CO_2 was then heated to 35 °C to reach supercritical conditions. The pressure range tested was 90–200 bar. The cell was heated to the same temperature as that of the pump using heating tape and the temperature of the optical cell was controlled using a separate PID temperature control unit. Starting at a low constant pressure, the absorbance at $\lambda = 280$ nm of CBZ was measured as a function of time until equilibrium was reached. Equilibrium was taken at the point where the absorbance values at $\lambda = 280$ nm remained constant. The pressure was increased by increments of 10 bar and the absorbances were measured at each pressure until equilibrium. The final equilibrium absorbance was determined when an increase in pressure did not affect absorbance, which denoted the point at with all the CBZ in the cell was solubilized. The graphical method for determining the equilibrium solubility point from a plot of absorbance as a function of pressure is depicted in Fig. 2 for 0.2 mg CBZ loaded into the optical cell. As seen from Fig. 2, an increase in pressure causes an increase in

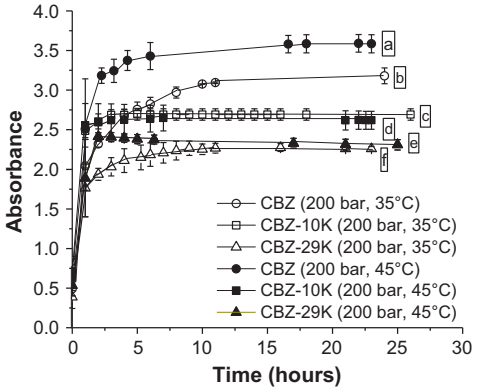

Fig. 3. Absorbance of CBZ ($\lambda = 280$ nm) as a function of time in the absence and presence of PVP 10 K and 29 K at 200 bar and 35 or 45 °C (mean ± S.E). The labels denote (a) CBZ (200 bar, 45 °C), (b) CBZ (200 bar, 35 °C), (c) CBZ-10 K (200 bar, 35 °C), (d) CBZ-10 K (200 bar, 45 °C), (e) CBZ-29 K (200 bar, 45 °C), and (f) CBZ-29 K (200 bar, 35 °C). Standard deviation bars are shown based on duplicate experiments.

the absorbance of CO_2, and at the solubility point there is a sharp change in the slope. The slight increase in absorbance above this point with increasing pressure is due to changes in molar absorptivities. The changes in the spectral shifts are polarizability driven and occur because of the dispersion forces between solute and solvent (Ngo et al., 2001; Rice et al., 1995). As the focus of this paper is to determine the solute partitioning in $scCO_2$ in the presence of polymer, all the measurements were performed at a fixed pressure (200 bar) where the solute was completely dissolved, thus pressure dependent changes in absorbance of CBZ did not have to be accounted for.

To determine $scCO_2$/PVP partitioning, CBZ absorbance was measured in the CO_2 phase as a function of time over a period of 24 h at a constant pressure of 200 bar and 35 or 45 °C. CBZ was loaded at 0.3 mg into the optical cell, which provided complete solubility in $scCO_2$. Partition coefficients with PVP 10 K and PVP 29 K were conducted at a 1:1 mass ratio of CBZ to PVP. The absorbance of CBZ starting at time zero in the presence of PVP, and as a function of CO_2 pressure, was measured by the same procedure described above. In all cases the cell was depressurized over a 15 min timeframe.

2.3. PVP characterization by scanning electron microscopy (SEM)

The size and morphology of the pure component and the binary PVP samples were observed by SEM (JEOL 5900 LV system, Tokyo, Japan) at 20 kV accelerating voltage using back scattered energy. Samples were sputter coated with gold (Au) at approximately 200 Å thickness.

3. Results and discussion

The solubility of CBZ in $scCO_2$ at 35 °C was 2.4, 3.4, and 5.4 ($\times 10^{-6}$ mol mol^{-1}) at 100, 120, and 200 bar, respectively. These values are in agreement with Bettini et al. (2001), which further validates our experimental system and procedures. The absorbance versus time profiles of CBZ at 200 bar and 35 or 45 °C in the absence and presence of PVP 10 K and 29 K are shown in Fig. 3. The initial rate of dissolution, taken as the slope from 0 to 30 min, was similar under all conditions. In the absence of PVP, CBZ absorbance reached equilibrium faster at 45 °C than at 35 °C (6 and 10 h, respectively), indicating faster total dissolution at the higher temperatures where mass transfer in CO_2 is greatest due to lower kinematic viscosity. Given that all of the CBZ was soluble at both temperatures, the difference in the equilibrium absorbance values is attributed to different CBZ molar absorptivities (a_D) at these two temperatures. Absorptivity values calculated by Beer's law ($a_D = A_{280\,nm}\, b^{-1} (x_D^{CO_2})^{-1}$, where $A_{280\,nm}$ is the equilibrium absorbance value, b is the length of the light path and $x_D^{CO_2}$ is the CBZ mole fraction in $scCO_2$) were 78,091 and 82,476 mol mol^{-1} cm^{-1} at 35 and 45 °C, respectively. The CO_2 densities used in the calculations of a_D were computed from the Peng–Robinson equation of state; 0.87 and 0.81 g ml^{-1} at 200 bar and 35 or 45 °C, respectively.

Table 1
In situ CBZ loading in PVP and $scCO_2$/PVP partition coefficients (mole fraction basis; Eq. (4)) as a function of temperature and PVP MW at 200 bar.

Sample[a]	T (°C)	*In situ* loading (wt%)	K_D (10^3)
CBZ + PVP 10 K[b]	35	15.9 ± 3.1	12.7 ± 3.7
	45	27.8 ± 3.9	31.8 ± 6.2
CBZ + PVP 29 K[b]	35	29.4 ± 0.9	31.7 ± 1.5
	45	37.8 ± 0.2	49.8 ± 0.3

[a] Below CBZ solubility limit under all conditions.
[b] Equal mass of CBZ and PVP.

In presence of PVP, the equilibrium absorbance values of CBZ in CO_2 were reduced as CBZ partitioned into the PVP phases. The fact that the equilibrium absorbance was reached at shorter times in the presence of PVP indicates that, once solubilized in $scCO_2$, CBZ quickly partitioned into the PVP phases. Hence, CBZ dissolution in $scCO_2$ was the rate-limiting step for PVP partitioning. In order to quantify the partitioning of the drug in the presence of the polymers, we calculated the mole fraction partition coefficients of the drug between the CO_2 and PVP phases from the following equations.

$$m_D^{CO_2} = M_D \frac{A^1_{280\,nm}}{A^2_{280\,nm}} \quad (1)$$

$$m_D^{PVP} = M_D - m_D^{CO_2} = M_D \left(1 - \frac{A^2_{280\,nm}}{A^1_{280\,nm}}\right) \quad (2)$$

$$x_D^{PVP} = \frac{m_D^{PVP}/MW_D}{m_{PVP}/MW_{N\text{-}VP}} \quad (3)$$

$$K_D = \frac{x_D^{PVP}}{x_D^{CO_2}} \quad (4)$$

Eq. (1) relates the mass of drug (D, CBZ) in CO_2 ($m_D^{CO_2}$) to the total mass of drug added (M_D) and the absorbance values in the absence ($A^1_{280\,nm}$) and presence ($A^2_{280\,nm}$) of PVP. The mass of drug partitioned into PVP (m_D^{PVP}, Eq. (2)) is the difference between M_D and $m_D^{CO_2}$, and the mole fraction of drug in PVP (x_D^{PVP}, Eq. (3)) was calculated on an N-vinylpyrrolidone monomer basis with molecular weight $MW_{N\text{-}VP}$. The drug partition coefficient was calculated on a mole fraction basis (K_D, Eq. (4)), with $x_D^{CO_2}$ calculated as described above based on molar adsorptivity.

$ScCO_2$/PVP partition coefficients are shown in Table 1. ANOVA at α 0.05 was used to determine whether the means were statistically different. The p-value of 0.0027 suggested that at least one mean was significantly different than the other. The values were further analyzed by the Tukey Kramer HSD test to determine the differences among the means. The results indicated that the PVP 29 K–CBZ mixture (45 °C, 200 bar) with a K_D value of $49.8 \pm 0.3 \times 10^3$ and PVP 10 K–CBZ mixture (35 °C, 200 bar) with a K_D value of $12.7 \pm 3.7 \times 10^3$ were significantly different. There was no statistical difference between the K_D values of PVP 10 K–CBZ (45 °C, 200 bar) and 29 K-CBZ (35 °C, 200 bar).

The CBZ partition coefficient and *in situ* loadings in PVP increased with both temperature and PVP molecular weight (Table 1). For $scCO_2$, increasing temperature reduces solvent strength (lower density) and increases mass transfer. Experiments were conducted below the CBZ solubility limit; therefore, changes in solvent strength did not cause CBZ to precipitate.

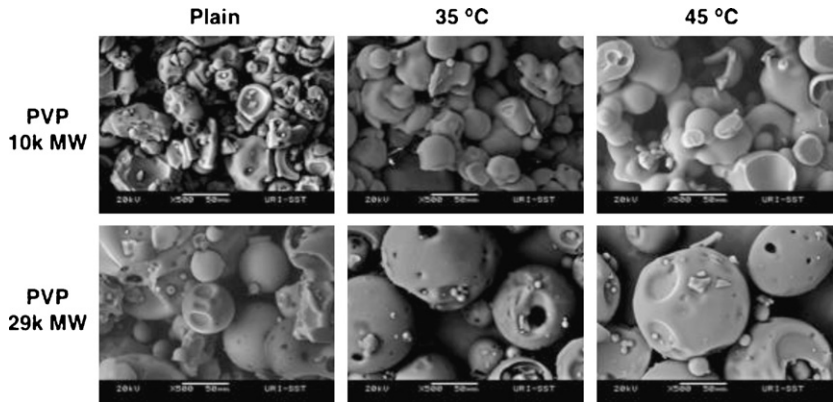

Fig. 4. Representative SEM micrographs of plain PVP (no CO_2 treatment) and PVP treated at 200 bar CO_2 and 35 or 45 °C in the absence of CBZ. PVP 10 K showed plasticization and interparticle fusion while PVP 29 K showed slight swelling.

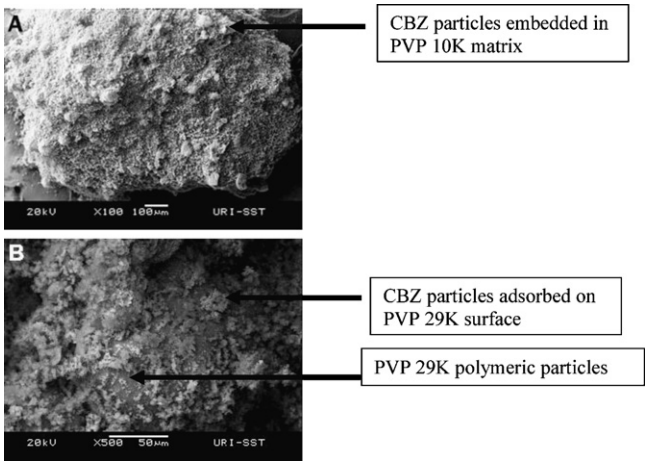

Fig. 5. Representative SEM micrographs of solid PVP–CBZ dispersions after $scCO_2$ treatment at *X* bar and *Y* °C. (A) PVP 10 K–CBZ depicting CBZ particles entrapped in PVP. (B) PVP 29 K–CBZ depicting CBZ particles adsorbed onto PVP particles.

Weaker solvent–solute interactions coupled with greater diffusivity increased the rate and extent of CBZ partitioning into the PVP phases at higher temperatures.

Within the solid phase, morphological changes in PVP, as most amorphous polymers, is dependent on polymer MW and CO_2 solvent strength and diffusivity. SEM micrographs show that increasing temperature from 35 to 45 °C at 200 bar enhanced the plastizication and degree of interparticle fusion for PVP 10 K (Fig. 4). Plasticization and fusion imply that there was an increased segmental mobility of the PVP 10 K chains. This increased mobility likely enhanced the diffusion of CBZ molecules into its matrix. Hence, greater plasticization of PVP 10 K appears to yield greater CBZ partitioning, consistent with previous observations of solute partitioning from $scCO_2$ into polymer phases (Yeo and Kiran, 2005). It is important to note that the SEM micrographs depict PVP structure after $scCO_2$ treatment and depressurization. Zhang et al. (1997) have shown that $scCO_2$ at 103.4 bar and 35 °C can swell PVP 65 K by 15%. While we did not measure swelling, the lower molecular weight PVPs used in this study coupled with the higher pressures would likely lead to greater swelling. Therefore, during CBZ partitioning the PVPs had a greater free volume for diffusion. SEM micrographs of the depressurized PVP 10 K–CBZ mixtures showed CBZ microparticles entrapped within PVP particles (Fig. 5a). As seen in Fig. 4, the surface characteristics of the plain PVP 10 K treated with $scCO_2$ is smooth, distinctly manifesting the fusion between the molecules because of plasticization. However, for PVP 10 K treated with $scCO_2$ in the presence of drug particles (Fig. 5), the surface is altered by protrusion of particles. Although the system is ternary, upon depressurization, the drug particles precipitate and get entrapped in PVP 10 K and because the mobility of the chains, the drug particles get embedded in the PVP 10 K matrix (Fig. 5a).

In PVP 29 K, little plasticization and no interparticle fusion were observed (Fig. 4). In addition the, PVP 29 K microparticles were also porous, which allowed CBZ to diffuse into the particles as well as on the surface of the particles leading to greater partitioning of drug. In contrast pores were not observed for PVP 10 K (Fig. 4). Hence, additional surface area was provided by the PVP 29 K particles relative to PVP 10 K. Fig. 5b illustrates surface adsorption of CBZ microparticles onto PVP 29 K rather than CBZ microparticle entrapment, as observed for PVP 10 K (Fig. 5a). For PVP 29 K, the polymer by itself shows a smooth superficial appearance marked by the presence of pores (Fig. 4). Upon depressurization, as PVP 29 K does not fuse but only swells, the drug particles tend to get deposited on the surface and within the porous cavities of the polymer.

These comparisons suggest that CBZ partitioning to PVP 29 K was driven primarily by surface adsorption, which can occur on both the inner and outer microparticle surfaces, as opposed to CO_2-enhanced CBZ diffusion within the polymer matrix. Hence, we observed that CBZ partitioning is controlled by plasticization and absorption for PVP 10 K, and surface adsorption for PVP 29 K.

It is important to point out that greater partitioning of CBZ into PVP 29 K did not translate into greater aqueous dissolution of CBZ after processing in our previous work. Only CBZ mixed with PVP 10 K showed an increased aqueous dissolution of CBZ (Ugaonkar et al., 2007). This phenomenon is explained by the classical studies conducted by Higuchi et al. (1965) and Higuchi (1967) where they have demonstrated that when the sample containing drug and the polymer are exposed to water, both the components dissolve at rates proportional to their solubilities and diffusion coefficients. The dissolution rate of the lesser dissolving component (CBZ) is then determined by the faster dissolving component (PVP). Further, water penetration, polymer swelling, drug dissolution and diffusion, and matrix erosion are important steps that occur during the drug dissolution process from a water-soluble matrix (Colombo et al., 1996). $ScCO_2$ treatment plasticizes PVP 10 K (as evident by intermolecular fusion in Fig. 4), which aided the erosion of PVP 10 K matrix and thereby enhanced the dissolution of CBZ observed from PVP 10 K. In contrast, PVP 29 K had a higher MW and did not plasticize, which did not aid its erosion and yielded a higher viscosity during dissolution relative to PVP 10 K.

4. Conclusions

The present work describes the *in situ* partitioning behavior of CBZ in $scCO_2$. The findings suggest that for the lower molecular weight PVP 10 K, CBZ partitioning was primarily governed by PVP plasticization and subsequent CBZ diffusion whereas for the higher molecular weight PVP 29 K, surface adsorption of CBZ on PVP 29 K was a key factor. The overall magnitude of CBZ partitioning in PVP 29 K was greater than in PVP 10 K, which suggests that, for these two PVP samples studied, surface adsorption yielded greater CBZ partitioning and loading (weight basis). The study also underscores the fact that greater CBZ partitioning into PVP phases does not translate to corresponding increases in the dissolution rate of CBZ in aqueous medium. Corresponding SEM images reveal that the nature of CBZ partitioning embedded in PVP 10 K matrix as opposed to surface adsorption in the case of PVP 29 K, determine the enhancement of aqueous dissolution as dissolution is primarily carrier controlled for systems where the carrier (PVP) has greater aqueous solubility than the solute (CBZ). Finally, the study demonstrates a facile method to quantifying drug partitioning in a ternary supercritical–drug–polymer system.

Acknowledgements

This work was funded in part by the National Science Foundation (Grant No. CHE 0715003). The authors wish to thank the Sensors and Surface Technology Partnership at the University of Rhode Island for the use of their SEM facility.

References

Bettini, R., Bonassi, L., Castoro, V., Rossi, V., Zema, L., Gazzaniga, A., Giordano, F., 2001. Solubility and conversion of carbamazepine polymorphs in supercritical carbon dioxide. Eur. J. Pharm. Sci. 13, 281–286.

Colombo, P., Bettini, R., Santi, P., Ascentiis, A.D., Peppas, N.A., 1996. Analysis of the swelling and release mechanisms from drug delivery systems with emphasis on drug solubility and water transport. J. Control. Release 39, 231–237.

Craig, D., Royall, P., Kett, V., Hopton, M., 1999. The relevance of the amorphous state to pharmaceutical dosage forms: glassy drugs and freeze dried systems. Int. J. Pharm. 179, 179–207.

El-Zein, H., Riad, L., El-Bary, A.A., 1998. Enhancement of carbamazepine dissolution: in vitro and in vivo evaluation. Int. J. Pharm. 168, 209–220.

Guney, O., Akgerman, A., 2002. Synthesis of controlled release products in supercritical medium. AIChE J. 48, 856–866.

Hancock, B.C., Shamblin, S., Zografi, G., 1995. Molecular mobility of amorphous pharmaceutical solids below their glass transition temperatures. Pharm. Res. 12, 799–806.

Hancock, B.C., Zografi, G., 1997. Characteristics and significance of the amorphous state in pharmaceutical systems. J. Pharm. Sci. 86, 1–12.

Higuchi, W.I., Mir, N.A., Desai, S.J., 1965. Dissolution rates of polyphase system. J. Pharm. Sci. 54, 1405–1410.

Higuchi, W.I., 1967. Diffusional models useful in biopharmaceutics. J. Pharm. Sci. 56, 315–324.

Hyatt, J.A., 1984. Liquid and supercritical carbon dioxide as organic solvents. J. Org. Chem. 49, 5097–5101.

Kazarian, S.G., Brantley, N.H., West, B.L., Vincent, M.F., Eckert, C.A., 1997. In situ spectroscopy of polymers subjected to supercritical CO_2: plasticization and dye impregnation. Appl. Spectrosc. 51, 491–494.

Kazarian, S.G., 2000. Polymer processing with supercritical fluids. Polym. Sci. Ser. C 42, 78–101.

Kazarian, S.G., 2004. Supercritical Fluid Impregnation of Polymers for Drug Delivery, Supercritical Fluid Technology for Drug Product Development. Marcel and Dekker, New York.

Kazarian, S.G., Martirosyan, G.G., 2002. Spectroscopy of polymer/drug formulations processed with supercritical fluids: in situ ATR-IR and Raman study of impregnation of ibuprofen into PVP. Int. J. Pharm. 232, 81–90.

Kikic, I., Vecchione, F., 2003. Supercritical impregnation of polymers. Curr. Opin. Solid State Mater. Sci. 7, 399–405.

Kikic, I., Lora, M., Cortesi, A., Sist, P., 1999. Sorption of CO_2 in biocompatible polymers: experimental data and qualitative interpretation. Fluid Phase Equilib. 158–160, 913–921.

McHugh, M.A., Krukonis, V.J., 1994. Supercritical Fluids Extraction. Butterworth-Heinemann, Boston.

Lőbenberg, R., Amidon, G.L., 2000. Modern bioavailability, bioequivalence and biopharmaceutics, classification system. New scientific approaches to international regulatory standards. Eur. J. Pharm. Biopharm. 50, 3–12.

Moneghini, M., Kikic, I., Voinovich, D., Perissutti, B., Filipovic-Grcic, J., 2001. Processing of carbamazepine-PEG 4000 solid dispersions with supercritical carbon dioxide: preparation, characterisation, and in vitro dissolution. Int. J. Pharm. 222, 129–138.

Mukhopadhyay, M., 2004. Phase Equilibrium in solid–liquid–supercritical fluid systems. Supercritical Fluid Technology for Drug Product Development. Marcel and Dekker, New York.

Nair, R., Gonen, S., Hoag, S.W., 2002. Influence of polyethylene glycol and povidone on the polymorphic transformation and solubility of carbamazepine. Int. J. Pharm. 240, 11–22.

Ngo, T.T., Bush, D., Eckert, C.A., Liotta, C.L., 2001. Spectroscopic measurement of solid solubility in supercritical fluids. AIChE J. 47, 2566–2572.

Rice, J.K., Niemeyer, E.D., Bright, F.V., 1995. Evidence for density-dependent changes in solute molar absorptivities in supercritical CO_2: impact on solubility determination practices. Anal. Chem. 67, 4354–4357.

Senčar-Božič, BožičP., Srčič, S., Knez, Z., Kerč, J., 1997. Improvement of nifedipine dissolution characteristics using supercritical CO_2. Int. J. Pharm. 148, 123–130.

Sethia, S., Squillante, E., 2004. Solid dispersion of carbamazepine in PVP K30 by conventional solvent evaporation and supercritical methods. Int. J. Pharm. 272, 1–10.

Shieh, Y.-T., Su, J.-H., Manivannan, G., Lee, P.H.C., Sawan, S.P., Spall, W.D., 1996. Interaction of supercritical carbon dioxide with polymers. I. Crystalline polymers. J. Appl. Polym. Sci. 59, 695–705.

Ugaonkar, S., Nunes, A.C., Needham, T.E., 2007. Effect of *n*-$scCO_2$ on crystalline to amorphous conversion of carbamazepine. Int. J. Pharm. 333, 152–161.

Yeo, S.-D., Kiran, E., 2005. Formation of polymer particles with supercritical fluids: a review. J. Supercrit. Fluid 34, 287–308.

Yoshioka, M., Hancock, B.C., Zografi, G., 1995. Inhibition of indomethacin crystallization in poly (vinylpyrrolidone) coprecipitates. J. Pharm. Sci. 84, 983–986.

Zhang, Y., Gangwani, K.K., Lemert, R.M., 1997. Sorption and swelling of block copolymers in the presence of supercritical fluid carbon dioxide. J. Supercrit. Fluid 11, 115–213.